DETECTION AIDED MULTISTATIC VELOCITY BACKPROJECTION FOR PASSIVE RADAR

Tegan Webster and Thomas Higgins

Radar Division, Naval Research Laboratory, Washington, DC, USA

ABSTRACT

This paper extends previous work to process and combine data from multiple bistatic pairs in a passive multistatic radar system. The previously presented Multistatic Velocity Backprojection (MVBP) combines and visualizes multistatic radar data. MVBP generates a six-dimensional data cube in position and velocity but does not provide a mechanism for detecting targets within the space. This paper discusses Detection Aided Multistatic Velocity Backprojection (DA-MVBP), a method for seeding MVBP with detections from individual bistatic pairs. DA-MVBP reduces the space through which it is necessary to search for targets in backprojected multistatic radar data and may result in enhanced parameter estimation and detection performance over traditional multilateration of detections. In this work DA-MVBP is applied to experimental passive multistatic radar data.

***Index Terms*—** multistatic radar, passive radar, backprojection, moving target indication, imaging

1. INTRODUCTION

Passive radar systems exploit dynamic signals from non-cooperative emitters, which differ substantially from traditional radar waveforms, to perform target detection, tracking, and imaging [1, 2, 3, 4]. Passive radar, however, often suffers from limited resolution due to wide antenna beamwidths and finite bandwidth of the signals of opportunity. Passive multistatic radar can achieve better localization in position and velocity by combining data from multiple bistatic pairs, utilizing multiple emitters of opportunity, multiple distributed receivers, or a combination of both [5, 6, 7, 8]. Previous work within the area of multistatic radar data processing and visualization includes theory for multistatic moving target detection [9, 10, 11, 12], multistatic imaging of a stationary scene [13, 14, 15], multistatic imaging of moving targets [16, 17, 18, 19], and the bistatic and multistatic ambiguity functions [20, 21, 22, 23].

Previously published work examined the application of Multistatic Velocity Backprojection (MVBP) to data obtained from passive multistatic radar experiments using WiMAX signals of opportunity [24]. MVBP combines range-Doppler processed data from individual bistatic pairs to visualize moving targets observed by multistatic radar systems and extends earlier work utilizing multistatic ambiguity analysis for moving target indication [16, 17, 18, 19]. The MVBP technique generates a six-dimensional data cube consisting of three dimensions of position and three dimensions of velocity but does not provide a mechanism for detecting targets within the position-velocity space.

This work describes a method for utilizing detections from individual bistatic pairs to significantly narrow the search space of MVBP. Denoted Detection Aided Multistatic Velocity Backprojection (DA-MVBP), the approach incorporates multilaterated positions and velocity estimates from individual bistatic pairs to form images of candidate moving targets. In many cases, multilateration and velocity estimation are capable of localizing moving targets. However, the output of the DA-MVBP algorithm may enhance parameter estimation and detection performance by facilitating the noncoherent combination of pre-detection data.

This paper first describes the method used to find and disambiguate detections from multistatic radar data in Section 2 and in Section 3 formulates the newly developed DA-MVBP by using the disambiguated detections to seed MVBP. DA-MVBP is applied to experimental data in Section 4 and Section 5 concludes the paper.

2. DETECTION PROCESSING OF EXPERIMENTAL PASSIVE BISTATIC DATA

DA-MVBP differs from MVBP by incorporating a method for seeding the search for moving targets within six-dimensional phase-space. Before application of DA-MVBP, detections are found in the data from each bistatic pair within the passive multistatic system. An approximation of the cross-ambiguity function is used to produce a range-Doppler map of the data from each bistatic pair [24]. Detections are then found from each coherent processing interval (CPI) of the processed bistatic data via the method illustrated in Figure 1.

A two-dimensional Cell-Averaging Constant False-Alarm Rate (CA-CFAR) detector is applied to the data in each range-Doppler map with a probability of false alarm of 10^{-6}. The two-dimensional CA-CFAR mask consists of rings of two guard cells and 10 training cells in range-Doppler space. The detections are centroided in both range and Doppler and must

This work was sponsored by the Office of Naval Research under the Naval Research Laboratory Base Program.

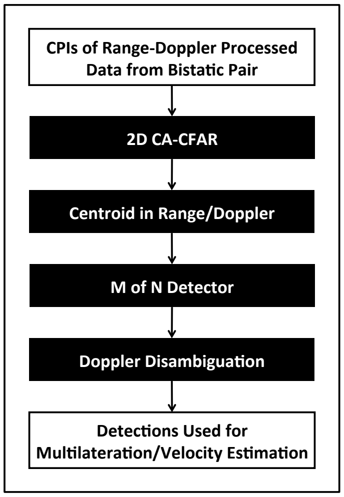

Fig. 1. Method for determining detections from each bistatic pair to be used for multilateration and velocity estimation.

be present in two subsequent CPIs. The remaining detections are disambiguated in Doppler. The low PRF WiMAX waveforms are velocity ambiguous but the high duty cycle of the signal (the downlink portion of the WiMAX frame constitutes 60% of the frame) results in the true velocity having the highest power in the cross-ambiguity function [24]. The disambiguated detections from each bistatic pair are used for multilateration and velocity estimation as described in Section 3.

3. DETECTION AIDED-MULTISTATIC VELOCITY BACKPROJECTION (DA-MVBP)

DA-MVBP reduces the volume of phase-space that must be searched to identify moving targets. This is achieved by extracting detections from individual bistatic pairs and using those detections for multilateration and velocity estimation.

For each CPI the bistatic ranges of the detections from all bistatic pairs in the multistatic system are used for multilateration, the output of which is a set of candidate positions. These positions, in conjunction with the bistatic Doppler measurements of each detection, are used for velocity estimation, yielding a set of candidate velocity vectors. The three-dimensional velocity vectors are then used to determine the three-dimensional slice of the six-dimensional position and velocity space that should be backprojected for a target at each of the candidate positions. Further assuming the value of one component of the position vector allows a two-dimensional position-position slice to be imaged via MVBP. Examining the backprojected image around the initial position and velocity estimates may facilitate higher-accuracy position and velocity estimates, which may be offset due to detection processing.

In the experimental results presented in this work only two transmitters of opportunity and a single receiver location could be utilized resulting in only two bistatic pairs. The transmitters, receivers, and targets of opportunity were not coplanar but the height and one component of the velocity vector of some of the targets were known, i.e., there were cars within the area of interest that were at a known height on a bridge and it was known that they were only moving across the bridge, i.e., their altitude was fixed. The method described above can still be employed to find a three dimensional position and velocity vectors by inputting the known height of a target into the multilateration step and inputting the known component of the velocity vector (zero in the vertical dimension) into the velocity estimation step as described in Sections 3.1 and 3.2.

3.1. Multilateration Using Two Bistatic Range Measurements and a Known Target Height

The following describes the process used to find a target position from two range measurements and a known third position dimension, in this case height. The method is similar to traditional multilateration as described in [25, 5] and elsewhere in the literature, but the expressions given in this section are tailored for a specific measurement scenario. Let the position of a receiver be denoted $\boldsymbol{p}_{\mathrm{R}} = [x_{\mathrm{R}}, y_{\mathrm{R}}, z_{\mathrm{R}}]^{\mathrm{T}}$ and the position of two transmitters, or emitters of opportunity, be denoted $\boldsymbol{p}_{\mathrm{A}} = [x_{\mathrm{A}}, y_{\mathrm{A}}, z_{\mathrm{A}}]^{\mathrm{T}}$ and $\boldsymbol{p}_{\mathrm{B}} = [x_{\mathrm{B}}, y_{\mathrm{B}}, z_{\mathrm{B}}]^{\mathrm{T}}$. Two bistatic range measurements from a possible target are given by $\boldsymbol{r} = [\rho_{\mathrm{A}}, \rho_{\mathrm{B}}]^{\mathrm{T}}$, where ρ_{A} is the range from the emitter at $\boldsymbol{p}_{\mathrm{A}}$ to the target to the receiver at $\boldsymbol{p}_{\mathrm{R}}$. To multilaterate detections from the passive bistatic experiment described in this paper, the bistatic range was found by adding the direct path distance, from the emitter of opportunity to the receiver, to the bistatic range delta measurement, obtained directly from the time difference of arrival at the receiver between the direct path signal and the reflected return.

Define

$$\boldsymbol{S} = \begin{bmatrix} x_{\mathrm{R}} - x_{\mathrm{A}} & y_{\mathrm{R}} - y_{\mathrm{A}} \\ x_{\mathrm{R}} - x_{\mathrm{B}} & y_{\mathrm{R}} - y_{\mathrm{B}} \end{bmatrix} \tag{1}$$

and

$$\boldsymbol{d} = \frac{1}{2} \begin{bmatrix} \rho_{\mathrm{A}}^2 + ||\boldsymbol{p}_{\mathrm{R}}||^2 - ||\boldsymbol{p}_{\mathrm{A}}||^2 \\ \rho_{\mathrm{B}}^2 + ||\boldsymbol{p}_{\mathrm{R}}||^2 - ||\boldsymbol{p}_{\mathrm{B}}||^2 \end{bmatrix}, \tag{2}$$

where $||\cdot||$ is the Euclidean norm, so that the multilaterated position $\boldsymbol{p} = [x, y, z]^{\mathrm{T}}$ corresponding to the given bistatic range measurements can be written as

$$\boldsymbol{p} = \begin{bmatrix} \left(\boldsymbol{S}^{-1}\boldsymbol{d}\right)^{\mathrm{T}} - \left(\boldsymbol{S}^{-1}\boldsymbol{r}\right)^{\mathrm{T}} \rho_{\mathrm{R}} & z \end{bmatrix}^{\mathrm{T}} \tag{3}$$

where ρ_{R} is the still unknown distance from the receiver to the target and z is the known height of the target.

The distance ρ_{R} can be found by calculating the quantities

$$\boldsymbol{a} = \boldsymbol{S}^{-1}\boldsymbol{d}, \tag{4}$$

and

$$\boldsymbol{b} = \boldsymbol{S}^{-1}\boldsymbol{r} \tag{5}$$

in (3) so that

$$\begin{bmatrix} x \\ y \end{bmatrix} = \begin{bmatrix} \boldsymbol{a}(1) + \boldsymbol{b}(1)\rho_{\mathrm{R}} \\ \boldsymbol{a}(2) + \boldsymbol{b}(2)\rho_{\mathrm{R}} \end{bmatrix}. \tag{6}$$

Rewriting the definition of ρ_{R} yields

$$\begin{aligned}\rho_{\mathrm{R}}^2 =&(x - x_{\mathrm{R}})^2 + (y - y_{\mathrm{R}})^2 + (z - z_{\mathrm{R}})^2 \\ =&x^2 - 2x_{\mathrm{R}}x - x_{\mathrm{R}}^2 + y^2 - 2y_{\mathrm{R}}y - y_{\mathrm{R}}^2 + (z - z_{\mathrm{R}})^2 \\ =&(\boldsymbol{a}(1) + \boldsymbol{b}(1)\rho_{\mathrm{R}})^2 - 2x_{\mathrm{R}}(\boldsymbol{a}(1) + \boldsymbol{b}(1)\rho_{\mathrm{R}}) - x_{\mathrm{R}}^2 \\ &+ (\boldsymbol{a}(2) + \boldsymbol{b}(2)\rho_{\mathrm{R}})^2 - 2y_{\mathrm{R}}(\boldsymbol{a}(2) + \boldsymbol{b}(2)\rho_{\mathrm{R}}) - y_{\mathrm{R}}^2 \\ &+ (z - z_{\mathrm{R}})^2 \end{aligned} \tag{7}$$

and (7) can be rearranged to obtain

$$0 = \rho_{\mathrm{R}}^2\alpha + \rho_{\mathrm{R}}\beta + \gamma \tag{8}$$

where

$$\begin{aligned}\alpha =&\boldsymbol{b}(1)^2 + \boldsymbol{b}(2)^2 - 1 \\ \beta =& - 2\boldsymbol{a}(1)\boldsymbol{b}(1) - 2\boldsymbol{a}(2)\boldsymbol{b}(2) + 2\boldsymbol{b}(1)x_{\mathrm{R}} + 2\boldsymbol{b}(2)y_{\mathrm{R}} \\ \gamma =&\boldsymbol{a}(1)^2 + \boldsymbol{a}(2)^2 - 2\boldsymbol{a}(1)x_{\mathrm{R}} - 2\boldsymbol{a}(2)y_{\mathrm{R}} - x_{\mathrm{R}}^2 - y_{\mathrm{R}}^2 \\ &+ (z - z_{\mathrm{R}})^2. \end{aligned} \tag{9}$$

Solving for the roots of (8) yields two solutions, $\rho_{\mathrm{R}+}$ and $\rho_{\mathrm{R}-}$, so that there are also two possible solutions for the position corresponding to the given range measurements $\boldsymbol{r}$

$$\boldsymbol{p}_1 = \begin{bmatrix} \boldsymbol{a}^{\mathrm{T}} - \boldsymbol{b}^{\mathrm{T}}\rho_{\mathrm{R}+} & z \end{bmatrix}^{\mathrm{T}} \tag{10}$$

$$\boldsymbol{p}_2 = \begin{bmatrix} \boldsymbol{a}^{\mathrm{T}} - \boldsymbol{b}^{\mathrm{T}}\rho_{\mathrm{R}-} & z \end{bmatrix}^{\mathrm{T}}. \tag{11}$$

It may be possible to deghost the solutions using the look direction of the receiving antenna when the receiving antenna is not omnidirectional.

3.2. Velocity Estimation Using Two Bistatic Doppler Measurements and One Known Component

This section describes estimation of a three-dimensional velocity vector using two bistatic Doppler measurements, a known third component of the velocity vector, and the multilaterated position obtained using the process described in 3.1. Unlike the previously described multilateration, estimation of a three-dimensional velocity vector using two measurements and a known third component reduces to solving a simple system of two equations, reproduced in this paper for completeness.

Let $\boldsymbol{\nu} = [\nu_{\mathrm{A}}, \nu_{\mathrm{B}}]^{\mathrm{T}}$ denote two bistatic velocity measurements corresponding to a possible target at position $\boldsymbol{p}$, where ν_{A} is the velocity measurement from the bistatic pair consisting of the emitter at $\boldsymbol{p}_{\mathrm{A}}$ and similarly for ν_{B}. The bistatic velocity measurements are obtained by multiplying the corresponding measured bistatic Doppler frequencies by the quantity c_0/f_c where f_c is the carrier frequency of the radar waveform or signal of opportunity. Define

$$\boldsymbol{S_v} = \begin{bmatrix} \frac{x-x_{\mathrm{A}}}{||\boldsymbol{p}_{\mathrm{A}}-\boldsymbol{p}||} + \frac{x-x_{\mathrm{R}}}{||\boldsymbol{p}_{\mathrm{R}}-\boldsymbol{p}||} & \frac{y-y_{\mathrm{A}}}{||\boldsymbol{p}_{\mathrm{A}}-\boldsymbol{p}||} + \frac{y-y_{\mathrm{R}}}{||\boldsymbol{p}_{\mathrm{R}}-\boldsymbol{p}||} \\ \frac{x-x_{\mathrm{B}}}{||\boldsymbol{p}_{\mathrm{B}}-\boldsymbol{p}||} + \frac{x-x_{\mathrm{R}}}{||\boldsymbol{p}_{\mathrm{R}}-\boldsymbol{p}||} & \frac{y-y_{\mathrm{B}}}{||\boldsymbol{p}_{\mathrm{B}}-\boldsymbol{p}||} + \frac{y-y_{\mathrm{R}}}{||\boldsymbol{p}_{\mathrm{R}}-\boldsymbol{p}||} \end{bmatrix} \tag{12}$$

so that

$$\boldsymbol{\nu} = \boldsymbol{S_v v} \tag{13}$$

and the velocity estimate is represented by the expression

$$\boldsymbol{v} = \begin{bmatrix} \left(\boldsymbol{S_v}^{-1}\boldsymbol{\nu}\right)^{\mathrm{T}} & v_z \end{bmatrix}^{\mathrm{T}} \tag{14}$$

where $\boldsymbol{v} = [v_x, v_y, v_z]^{\mathrm{T}}$ is the velocity estimate for a target at position $\boldsymbol{p}$ and v_z is the known component of the velocity vector.

4. EXPERIMENTAL RESULTS

This section applies the processing method described in Sections 2-3 to passive multistatic experimental radar data. DA-MVBP is used to localize, in position and velocity space, moving vehicles using two WiMAX towers as illuminators of opportunity. The two towers each transmit a different WiMAX communications signal with a center frequency of 2.667 GHz and a bandwidth of 10 MHz. The data consists of 2 CPIs each composed of 50 WiMAX frames. Table 1 gives the measured bistatic range and bistatic range delta from each tower to the vehicles and back to the receiver.

Table 1. Measured Bistatic Ranges and Bistatic Range Deltas for the Moving Vehicles

Tower	Measured Bistatic Range (km)	Measured Bistatic Range Delta (km)
Tower 1	9.71	5.35
Tower 2	6.86	3.62

Figure 2 presents the range-Doppler estimates from one CPI of passive experimental data from the two bistatic pairs. Clutter cancellation has been applied to the data. The two subfigures show the same extent in bistatic range delta and bistatic Doppler frequency and the red circles denote moving vehicles that appear at ranges and Doppler shifts that will be visualized via DA-MVBP later in this section.

The data is next processed according to the method described in Section 2. The detections output by the two-dimensional CA-CFAR detector from a single CPI are centroided in range and Doppler. The centroided detections are then passed through a "2 of 2" detector that utilizes a sliding window and the remaining detections are disambiguated in velocity. In the specific example shown in this paper the

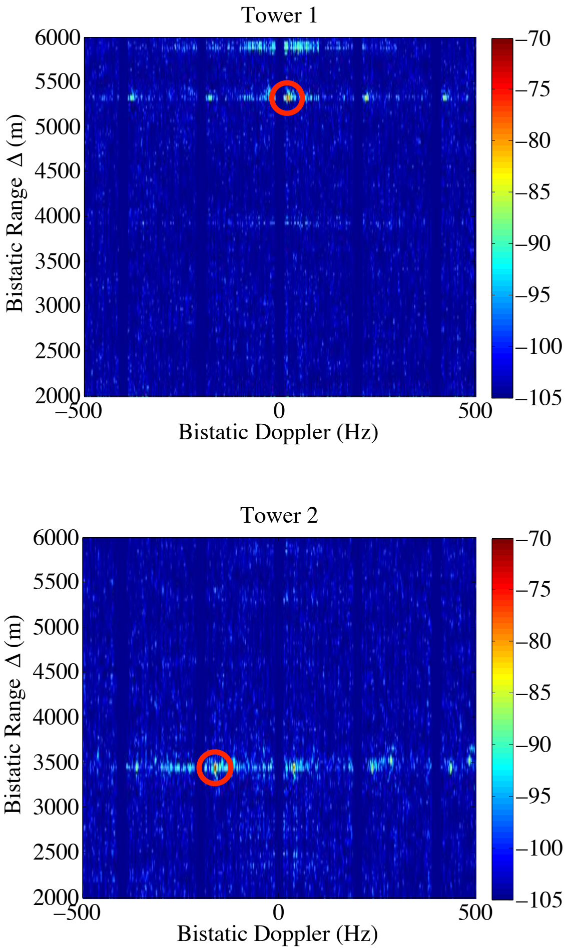

Fig. 2. Range-Doppler maps produced via QFTMF of the passive experimental data including moving vehicles from each bistatic pair.

detections are velocity ambiguous due to the signals of opportunity utilized by the passive experiment. The disambiguated detections from each CPI of data are then used for multilateration and velocity estimation as described in Section 3 and the produced velocity vectors are utilized by DA-MVBP to visualize individual moving targets.

Next, the experimental data from the two bistatic pairs are back-projected in space and velocity via DA-MVBP. Although position and velocity estimates have been found from the data, these estimates are not the final product but are used to aid DA-MVBP. Many of the position estimates produced by the method described in Section 3 are ghost target locations and do not correspond to a true target. However, the candidate target locations can be used to reduce the search through position and velocity space by limiting the number of velocity vectors and the range of positions examined by DA-MVBP. Figure 3 displays a two-dimensional (range, cross-range) slice of the data cube formed by selecting the height ($z = 30$ m), known a priori in this example, and the estimated velocity vector consistent with a moving vehicle with a velocity magnitude of 14.74 m/s and an azimuth direction of 181.65^{o} (relative to the x-axis) in the x-y plane. A binary 20^{o} receive beampattern consistent with the receiver antenna beamwidth has been overlaid on the image and a red circle denotes the initial position estimate of the target.

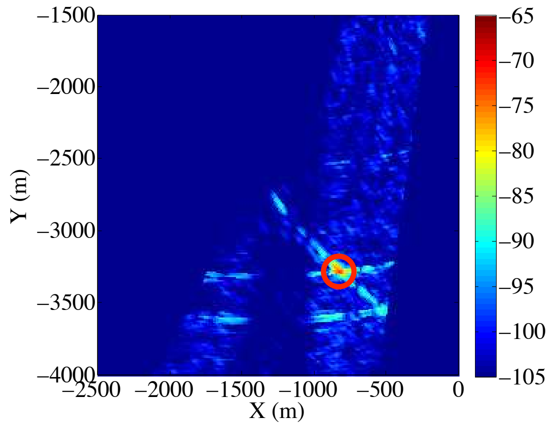

Fig. 3. Backprojection via DA-MVBP of a moving vehicle from passive multistatic experimental data collected using two WiMAX towers as illuminators of opportunity.

5. CONCLUSIONS

This paper discussed and experimentally demonstrated an extension to Multistatic Velocity Backprojection (MVBP), a previously presented method for processing and combining data from multiple bistatic pairs in a multistatic radar system. Detection Aided Multistatic Velocity Backprojection (DA-MVBP) uses position and velocity estimates to select the correct slice out of the full six-dimensional position and velocity space that can be produced via MVBP, thereby facilitating imaging of a moving target without (or with limited) prior knowledge of target parameters. DA-MVBP may also enable enhanced parameter estimation and detection performance over traditional multilateration of detections by using the initial position and velocity estimates to seed the search in phase-space for refined target position and velocity vectors, which will have a maximum value in the backprojected image. This process is currently being investigated to quantify the benefit of DA-MVBP.

6. REFERENCES

[1] H. D. Griffiths and C. J. Baker, “Passive coherent location radar systems. Part 1: Performance prediction,” *IEE Proceedings: Radar, Sonar and Navigation*, vol. 153, no. 3, pp. 153–159, 2005.

[2] C. J. Baker, H. D. Griffiths, and I. Papoutsis, "Passive coherent location radar systems. Part 2: Waveform properties," *IEE Proceedings: Radar, Sonar and Navigation*, vol. 153, no. 3, pp. 160–168, 2005.

[3] N. J. Willis and H. D. Griffiths, Eds., *Advances in Bistatic Radar*, SciTech Publishing, Raleigh, NC, 2007.

[4] J.E. Palmer, H.A Harms, S.J. Searle, and L.M. Davis, "DVB-T passive radar signal processing," *IEEE Trans. Signal Processing*, vol. 61, no. 8, pp. 2116–2126, Apr. 2013.

[5] M. Malanowski, "An algorithm for 3D target localization from passive radar measurements," in *Proc. of SPIE: Photonics Applications in Astronomy, Communications, Industry, and High-Energy Physics Experiments 2009*, Wilga, PL, May 2009, vol. 7502, pp. 75 021B–1–75 021B–6.

[6] K.S. Bialkowski, I V L Clarkson, and S.D. Howard, "Generalized canonical correlation for passive multistatic radar detection," in *2011 IEEE Statistical Signal Processing Workshop (SSP)*, June 2011, pp. 417–420.

[7] D. E. Hack, L. K. Patton, A. D. Kerrick, and M. A. Saville, "Direct cartesian detection, localization, and deghosting for passive multistatic radar," in *2012 IEEE 7th Sensor Array and Multichannel Signal Processing Workshop*, Hoboken, NJ, USA, June 2012, pp. 45–48.

[8] J.H.G. Ender, "A compressive sensing approach to the fusion of pcl sensors," in *2013 Proc. of the 21st European Signal Processing Conference (EUSIPCO)*, Sept. 2013, pp. 1–5.

[9] B. Himed, H. Bascom, J. Clancy, and M. C. Wicks, "Tomography of moving targets (TMT)," in *Proc. of SPIE*, Dec. 2001, vol. 4540, pp. 608–619.

[10] R. S. Adve, R. A. Schneible, M. C. Wicks, and R. McMillan, "Space-time adaptive processing for distributed aperture radars," in *2004 International Waveform Diversity and Design Conference*, Edinburgh, UK, Nov. 2004, pp. 1–5.

[11] I. Bradaric, G.T. Capraro, D.D. Weiner, and M.C. Wicks, "Multistatic radar systems signal processing," in *2006 IEEE Radar Conference*, Verona, New York, USA, Apr. 2006, p. 22.

[12] L. Landi and R. S. Adve, "Time-orthogonal-waveform-space-time adaptive processing for distributed aperture radars," in *2007 International Waveform Diversity and Design Conference*, Pisa, IT, June 2007, pp. 13–17.

[13] A. J. Devaney, "A filtered backpropagation algorithm for diffraction tomography," *Ultrasonic Imaging*, vol. 4, pp. 336–350, 1982.

[14] D. Colton and R. Kress, *Inverse Acoustic and Electromagnetic Scattering Theory*, Springer, Berlin, second edition, 1998.

[15] T. Varsolt, B. Yazici, and M. Cheney, "Wide-band pulse-echo imaging with distributed apertures in multi-path environments," *Inverse Problems*, vol. 24, no. 4, pp. 045013, Aug. 2008.

[16] M. Cheney and B. Borden, "Imaging moving targets from scattered waves," *Inverse Problems*, vol. 24, pp. 22, Oct. 2008.

[17] L. Wang, M. Cheney, and B. Borden, "Multistatic radar imaging of moving targets," in *2010 IEEE Radar Conference*, Washington, DC, USA, May 2010, pp. 391–396.

[18] T. Webster, L. Xu, and M. Cheney, "Antenna beam patterns in MIMO radar," in *2012 IEEE Radar Conference*, Atlanta, GA, USA, May 2012, pp. 332–337.

[19] T. Webster, M. Cheney, and E. L. Mokole, "Multistatic polarimetric radar data modeling and imaging of moving targets," *Inverse Problems*, vol. 30, no. 3, pp. 24, Feb. 2014.

[20] T. Tsao, M. Slamani, P. Varshney, D. Weiner, H. Schwarzlander, and S. Borek, "Ambiguity function for a bistatic radar," *IEEE Trans. on Aerospace and Electronic Systems*, vol. 33, no. 3, pp. 1041–1051, July 1997.

[21] G. San Antonio, D. R. Fuhrmann, and F. C. Robey, "Mimo radar ambiguity functions," *IEEE Journal of Selected Topics in Signal Processing*, vol. 1, no. 1, pp. 167–177, June 2007.

[22] T. Derham, S. Doughty, C. Baker, and K. Woodbridge, "Ambiguity functions for spatially coherent and incoherent multistatic radar," *IEEE Trans. on Aerospace and Electronic Systems*, vol. 46, no. 1, pp. 230–245, Jan. 2010.

[23] A. Guruswamy and R. Blum, "On a definition of the ambiguity function for non-coherent radars," in *2012 IEEE 7th Sensor Array and Multichannel Signal Processing Workshop*, Hoboken, NJ, USA, June 2012, pp. 141–144.

[24] T. Webster, T. Higgins, and A. K. Shackelford, "Multistatic velocity backprojection for visualizing simulated and experimental multistatic radar data," in *2014 IEEE Radar Conference*, Cincinnati, OH, May 2014, pp. 968–973.

[25] J. L. Gertz, "Mode S surveillance netting," Project Report ATC-120, MIT Lincoln Laboratory, Lexington, MA, Nov. 1983.